Multilayer Dielectric End-Fire Antenna With Enhanced Gain

Denise C. Lugo, *Student Member, IEEE*, Ramiro A. Ramirez, *Student Member, IEEE*, Jing Wang, *Member, IEEE*, and Thomas M. Weller, *Fellow, IEEE*

***Abstract*—The effect of a low permittivity cladding used in a multilayer end-fire dielectric rod antenna (DRA) design is studied in terms of return loss, gain, and half-power beamwidth (HPBW) in the extended Ku band (10–18 GHz). Gain improvement ranging from 4 to 7 dB, when compared to a single-layer design of the same length, is achieved using cladding permittivities between 1.6 and 2.6. For example, a cladding of $\varepsilon_r = 1.6$ leads to a peak gain increment of 4.5 dB at 18 GHz and a 20° HPBW reduction compared to the noncladded rod. It is also demonstrated that this design has the same maximum gain as a noncladded design that is 1.8 times longer. The cladding permittivity in the multilayer DRA can be adjusted to achieve peak performance at different frequencies within the band, while providing gain enhancement in the entire band without reducing the bandwidth.**

***Index Terms*—Additive manufacturing, dielectric rod antenna (DRA), end fire, Ku band, multilayer, rectangular waveguide.**

I. Introduction

DIELECTRIC rod antennas (DRAs) represent a viable option for ultra-wideband (UWB) end-fire systems when compared to conventional aperture horn antennas or tapered slot radiators. DRAs can often achieve performance that is similar to these alternative approaches accompanied not only with lighter weight, reduced volume, and small cross section, but also with low mutual coupling between single elements in array configurations [1]. These characteristics continue to generate interest in a wide variety of fields and applications such as satellite communications [2], radar systems [3], chip-to-chip communications [4], and millimeter-wave imaging [5], [6].

Several efforts have been made to enhance the performance of DRAs in the past decade. Improvements in gain have been studied using methods that modify the physical shape of the DRA [6], or by increasing the number of elements in end-fire array configurations [7]. Different feed networks have also been investigated, for example exciting the DRA with a tapered slot antenna or using the rod itself as a feed for reflector antennas, such as horns or parabolic dishes [8], [9]. More recent studies include substrate-integrated waveguide feed networks and embedded multilayer structures that avoid excitation of high-order modes [1], [10].

It is well known that gain enhancements in DRAs can be achieved by increasing the rod permittivity or the rod diameter. Increased gain is also possible with increased antenna length, although this may degrade other antenna parameters such as cross polarization and sidelobe levels (SLLs) [1]. Increasing the core diameter, on the other hand, may affect the operational bandwidth, since higher order modes are excited at frequencies where the diameter becomes much larger than the guided wavelength [1]. Gain improvements have been reported in [11] where two low permittivity dielectrics with a small refractive index difference are used along with a custom metal waveguide transition.

Additionally, the implementation of multiple dielectric layers in circular DRAs is used to improve the antenna bandwidth [12], [13].

In other types of antennas such as dipoles, variation of the substrate dielectric constant has been studied as a means to enhance the broadside gain [14].

The present work addresses the characterization and gain enhancement of a low-permittivity cladding in a DRA design with rectangular cross section, a concept initially presented in [15]. The multilayer DRA design is comprised of a high-permittivity core ($\varepsilon_r = 10.2$) encased in a low-permittivity cladding ($1.6 \leq \varepsilon_r \leq 2.6$). This letter demonstrates that the cladding permittivity can be strategically selected to provide a significant gain enhancement relative to a single-layer DRA of the same length, without reducing the operational bandwidth. Variations of the cladding permittivity are achieved by implementing commercially available additive manufacturing (AM) techniques, which are used to tune the peak gain in the extended Ku band (10–18 GHz). In particular, it is shown that a cladding of $\varepsilon_r = 1.6$ increases the antenna gain between 2.7 and 4.5 dB in the entire frequency range, which is comparable to a single-layer (noncladded) DRA that is 1.8 times longer. More generally, through simulation it is demonstrated that for the presented design a cladding permittivity to core permittivity ratio of 0.15 to 0.4 provides the best overall gain performance. In this range, the radiated fields along the antenna length are appropriately phased to maximize directionality without significant increase in the SLL.

II. Dielectric Rod Antenna Design and Fabrication

The geometry of a traveling wave rod antenna is usually formed by three sections: a feed taper which is inserted into the rectangular waveguide feed to gradually match the input impedance; a body gradient; and a constant height section to minimize the reflected surface wave [6], [16], [17]. For a DRA

Manuscript received May 28, 2018; revised August 12, 2018; accepted September 9, 2018. Date of publication September 19, 2018; date of current version November 29, 2018. This work was supported by the U.S. National Science Foundation under Grant ECCS-1509762. *(Corresponding author: Denise C. Lugo.)*

D. C. Lugo, R. A. Ramirez, and J. Wang are with the Electrical Engineering Department, University of South Florida, Tampa, FL 33620 USA (e-mail: deniselugo@mail.usf.edu; ramiror@mail.usf.edu; jingw@usf.edu).

T. M. Weller is with the Electrical Engineering and Computer Science Department, Oregon State University, Corvallis, OR 97331 USA (e-mail: tom.weller@oregonstate.edu).

Digital Object Identifier 10.1109/LAWP.2018.2871103

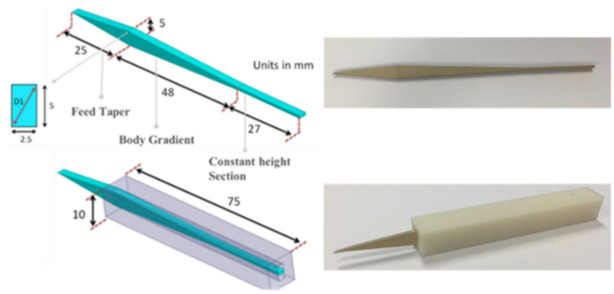

Fig. 1. Proposed multilayer DRA geometry and key dimensions, showing the inner core (top) and multilayer design (bottom).

with circular cross section, the diameter of the antenna D should satisfy the following equation to ensure that the fundamental mode (HE_{11}) is supported [9] and confined within the core [1]:

$$\frac{\lambda_0}{4} < D < \frac{0.626}{\sqrt{\varepsilon_r}}\lambda_0 \quad (1)$$

where λ_0 is the free space wavelength.

Since the DRA design in this letter utilizes a rectangular cross section, equivalence radii between the two geometries (i.e., rectangular and circular) are used as suitable approximation to satisfy (1) and (2) [15]. For a rectangle of 2:1 aspect ratio, its equivalent diagonal *D1* is then selected as 1.315 D according to [18]. The geometry of the multilayer antenna for the extended Ku band is depicted in Fig. 1. The antenna length determines the peak gain and the half-power beamwidth (HPBW), and in this type of antenna the total body length often falls between 3 λ_0 and 6 λ_0. As shown later in this letter, DRAs with shorter electrical length show less gain variation with frequency as compared to longer rods, and a short length thus makes it easier to isolate and analyze the effect of the cladding. In this design, a total length of 75 mm (3.5 λ_0 at the center frequency) was chosen as a baseline to study the effect of the cladding.

The DRA core was fabricated by laser cutting a Rogers RO3010 ($\varepsilon_r = 10.2$ and loss tangent $= 0.0035$) substrate, which is comparable in cost to Rogers laminates with lower dielectric constants. The cladding is fabricated as a separate hollow structure using fused deposition modeling (FDM) of acrylonitrile butadiene styrene (ABS) ($\varepsilon_r = 2.6$ and loss tangent $= 0.0052$). Two claddings were fabricated, one with 100% infill to achieve an effective cladding permittivity ε_r of 2.6 [15], and one with 50% honeycomb infill to achieve $\varepsilon_r = 1.6$ at 18 GHz. An attractive feature of the multilayer DRA design is its compatibility with three-dimensional (3-D) printing technology. A fully 3-D printed variation of this design was successfully implemented in the Ka band [19].

III. DRA Characterization and Measurements

The DRA performance was measured in an anechoic chamber with cladding permittivities of 1.6 and 2.6. The performance of the single-layer or noncladded design was also measured for comparison purposes. The measured peak gain and corresponding high frequency structure simulator (HFSS) simulation data are shown in Fig. 2(a). The multilayer antenna with $\varepsilon_r = 1.6$ cladding shows a significant gain improvement at all frequencies of interest compared to the noncladded antenna of the same length. The multilayer antenna peak gain is 16.24 dBi at 17.2 GHz, representing a 4.44 dB improvement with respect to the single-layer rod antenna. The multilayer design with a

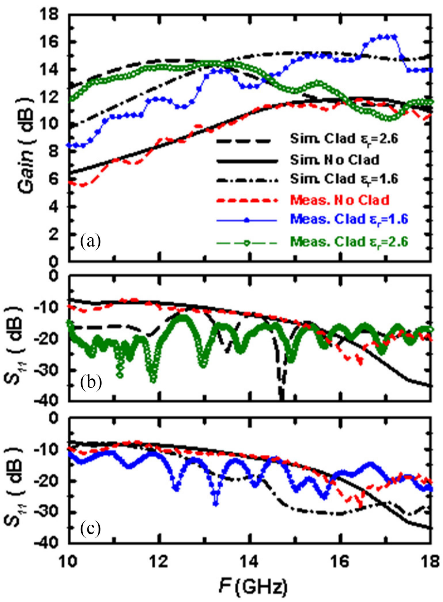

Fig. 2. Measured and simulated peak gain (a) and reflection coefficient (b, c) of the single and multilayer DRAs with different cladding permittivities.

$\varepsilon_r = 2.6$ cladding shows an enhanced gain in the low end of the Ku and a comparable gain beyond 15 GHz when compared to the noncladded rod performance. In this multilayer DRA, a 14.6 dBi band peak gain occurs at 12.2 GHz, representing a 4.8 dB gain increment. In all cases, the measured gain follows the simulated trend over frequency. The variations in the measured data can be attributed to the presence of the fixture stage, and the feeding metallic waveguide on the back of the antenna under test.

Fig. 2(b) presents a comparison of the measured and simulated return loss for the single- and multilayer DRAs with $\varepsilon_r = 2.6$ cladding while Fig. 2(c) shows the same comparison but with a cladding of $\varepsilon_r = 1.6$. In both cases, the multilayer designs have an improved return loss at the low end of the frequency band. For the multilayer DRAs, the return loss is greater than 10 dB across the entire frequency range.

The measured and simulated E-plane radiation patterns of the single- and multilayer DRAs with $\varepsilon_r = 2.6$ cladding at 12.2 GHz are presented in Fig. 3(a) and (b), respectively. The radiated fields are affected by the presence of the cladding, as the HPBW reduces from 61° to 22° in the multilayer design [15]. The end-fire cross-polarization discrimination is 47 dB for the single-layer DRA and 39 dB for the multilayer DRA at 12.2 GHz. Similarly, the measured and simulated E-plane radiation patterns at 17.2 GHz for the single- and multilayer DRAs with $\varepsilon_r = 1.6$ cladding are shown in Fig. 3(b) and (c), respectively. In this case, the HPBW reduces from 48° to 28° in the multilayer design. A measured front to back ratio of 26 dB is also achieved for the multilayer antenna. The end-fire cross-polarization discrimination is 43 and 38 dB for the single and multilayer DRAs, respectively.

The addition of the low permittivity cladding results in a peak gain increment, which can be attributed to two effects: 1) an increase in the effective permittivity and thus the electrical length of the antenna; and 2) an increase in the field confinement that reshapes the radiation pattern and results in higher directivity. The electric field magnitude of the single- and multilayer antennas with $\varepsilon_r = 2.6$ cladding is presented in Fig. 4. It can be

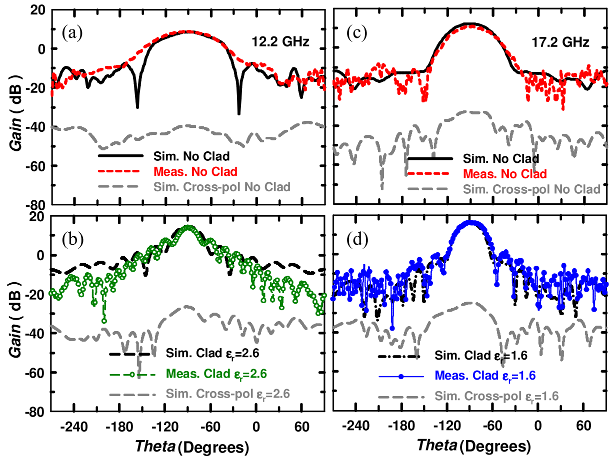

Fig. 3. Measured and simulated E-plane radiation pattern for the single (a) and multilayer (b) DRA with $\varepsilon_r = 2.6$ cladding at 12.2 GHz [15] and for the single (c) and multilayer (d) DRA with $\varepsilon_r = 1.6$ cladding at 17.2 GHz.

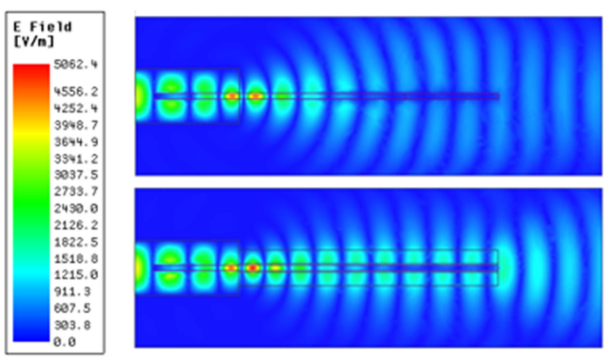

Fig. 4. Simulated E-field distribution at 17.2 GHz for the single (top), and multilayer (bottom) DRA with $\varepsilon_r = 2.6$ cladding.

observed that in the multilayer DRA there is a higher portion of the E-field radiated in the end-fire direction.

The 3-D radiation pattern of the single- and multilayer DRAs at 17.2 GHz with $\varepsilon_r = 1.6$ cladding is shown in Fig. 5(a) and (b), respectively. The corresponding E- and H-plane radiation patterns are plotted in Fig. 5(c) and (d) for the single- and multilayer DRAs, respectively. It can be seen that the symmetry of the radiation patterns in both planes are affected by the 2:1 core cross-section ratio. The differences in symmetry are more noticeable for the single-layer DRA.

Fig. 6 shows the simulated noncladded DRA peak gain versus frequency for different length increments (ΔL) of the core body gradient. The curve with the lowest gain ($\Delta L = 0$ mm) corresponds to the original design shown in Fig. 1 with no cladding. The gain versus frequency response of the multilayer DRA with $\varepsilon_r = 1.6$ cladding is included in the plot as a reference. As shown, an increment of at least 60 mm is required to match the gain of the multilayer antenna at the center frequency; this represents a 2.25× increase in the body gradient length and a 1.8× increase in the total DRA length.

For frequencies above 15 GHz, an increment of 120 mm or 3.5 times the body gradient is necessary to match the multilayer DRA gain. It can be seen in Fig. 6 that increasing the rod length increases the gain in a nonuniform way. For frequencies above 14 GHz, the gain slowly decays due to an increase in the SLL in the H-plane. Additionally, increasing the antenna length from $\Delta L = 0$ to 140 mm reduces the cross-polarization discrimination at 18 GHz from 44 to 34 dB.

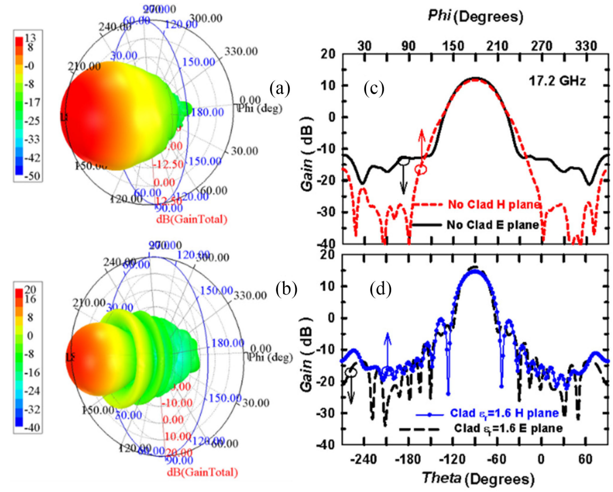

Fig. 5. Simulated far-field 3-D radiation pattern for the single (a) and multilayer (b) DRA. Simulated E- and H-plane radiation patterns of the single (c) and multilayer (d) DRA with $\varepsilon_r = 1.6$ cladding at 17.2 GHz.

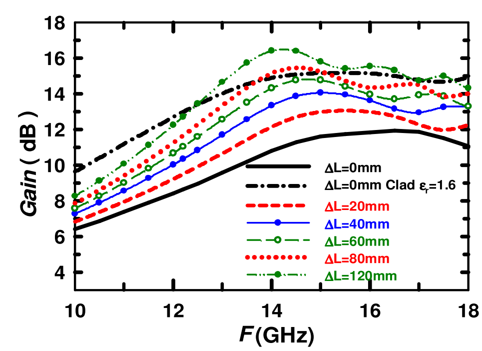

Fig. 6. Simulated gain versus frequency for different length increments of the body gradient in a single-layer DRA.

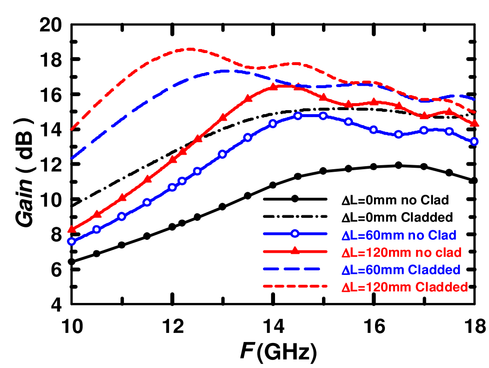

Fig. 7. Simulated gain versus frequency for different length increments of the body gradient in a single- and multilayer DRAs.

Fig. 7 presents the end-fire gain of the single- and multilayer DRAs with body gradient increments of 120, 60, and 0 mm (original design). The cladding permittivity considered in the multilayer DRA is 1.6. It is seen that the advantages of the cladding are scalable and consistent with different antenna lengths, providing significant gain increments when compared to a single-layer rod of the same length.

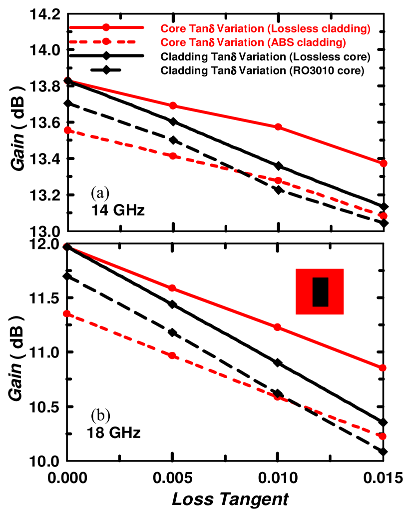

Fig. 8. Simulated end-fire gain versus loss tangent variation at (a) 14 GHz and (b) 18 GHz.

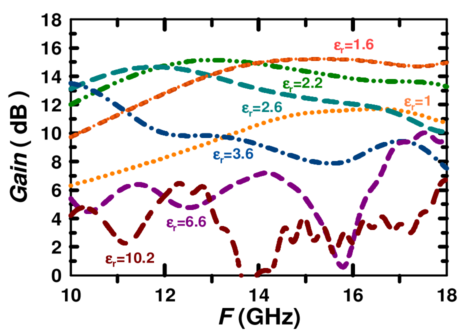

Fig. 9. Simulated gain versus frequency for different cladding permittivities.

IV. Parametric Study of the Cladding Properties

Fig. 8(a) and (b) shows the simulated effect of the loss tangent variation of the core and the cladding on the multilayer DRA gain at 14 and 18 GHz, respectively. The loss tangent (tanδ) values of the core and cladding varied from 0 to 0.015. Two sets of curves are plotted in Fig. 8, one where the cladding tanδ is varied (black curves) considering a Rogers RO3010 core and a lossless core, and one where the core tanδ is varied (red curves) considering an ABS cladding and a lossless cladding. At both frequencies, the difference between the dashed and solid red lines (ABS and lossless cladding) is larger than the difference between the dashed and solid black lines (RO3010 and lossless core). The data show that selecting a lossy material $(\tan\delta = 0.015)$ over a low loss material $(\tan\delta = 0.005)$ for the DRA cladding yields a ~0.5 dB reduction of the end-fire gain. Therefore, it can be concluded that the cladding loss tangent variation has a more significant effect on the multilayer DRA gain than the variation of the core loss tangent in the same range of values. This behavior can be attributed to the higher portion of the electromagnetic field that is radiated through the cladding in comparison to the core.

The simulated effects of varying the cladding permittivity on the gain of the multilayer DRA are presented in Fig. 9. The permittivity value is increased from $\varepsilon_r = 1$, which represents the absence of the cladding, up to a value of $\varepsilon_r = 10.2$ representing an identical material to that used for the core. Cladding permittivities between 1.6 and 2.6 provide a significant gain

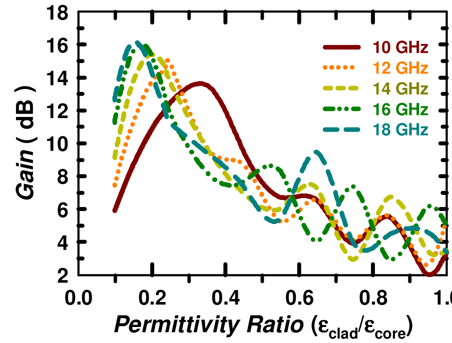

Fig. 10. Simulated gain versus cladding to core permittivity ratio for different frequencies.

enhancement when compared to the gain response of the noncladded antenna. The gain increment in these cases can range from 1.8 up to 7 dB over frequency. Moreover, the frequency of the end-fire peak gain can be tuned within the Ku band by adjusting the cladding dielectric constant. For cladding permittivity values between 2.6 and 3.6, the gain improvement is only present in the lower end of the frequency band, thus worsening the antenna performance for higher frequencies. For all frequencies within the band, the best performance of the proposed multilayer DRA is achieved when a low permittivity material $(1.6 \leq \varepsilon_r \leq 2.6)$ is utilized.

Fig. 10 shows the simulated end-fire peak gain versus the permittivity ratio $\varepsilon_{\text{clad}}/\varepsilon_{\text{core}}$. As in Fig. 9, the cladding permittivity was varied from 1 to 10.2 (the core permittivity value) corresponding to a permittivity ratio variation of 0.1 to 1. For all frequencies within the Ku band, the best performance of the proposed design is achieved when the cladding to core permittivity ratio lies between 0.15 and 0.4.

V. Conclusion

The effect of the cladding properties on the proposed multilayer DRA performance was studied. The multilayer DRA is formed by a high permittivity core $(\varepsilon_r = 10.2)$ with rectangular cross-section, surrounded by a low permittivity cladding $(1.6 \leq \varepsilon_r \leq 2.6)$. It is found that enhancements in gain and beamwidth can be achieved by providing the proper dielectric loading with respect to a single-layer design of the same length, without reducing the operational bandwidth. Simulated and measured data show that a low permittivity cladding can be utilized to tune the end fire peak gain to the desired frequency, from 12 GHz with $\varepsilon_r = 2.6$ cladding to 17 GHz with $\varepsilon_r = 1.6$ material. Physical changes to achieve the desired permittivity can be easily achieved by modifying the printing infill factor of the thermoplastic material. A multilayer DRA with a $\varepsilon_r = 1.6$ cladding shows a gain enhancement in the entire frequency band, with a peak gain improvement of 4.5 dB and 20° HPBW reduction at 17.2 GHz. The gain increment in the multilayer DRA with a cladding of $\varepsilon_r = 1.6$ can be achieved by a noncladded DRA only if the body-tapered length is increased more than 2.25 times. The multilayer DRA also increases the electric field confinement in the core, which translates to a higher potential packing density in an array configuration.

Acknowledgment

The authors wish to acknowledge the assistance and support of Rogers Corporation and Sciperio, Inc.

REFERENCES

[1] R. Kazemi, A. E. Fathy, and R. A. Sadeghzadeh, "Dielectric rod antenna array with substrate integrated waveguide planar feed network for wideband applications," *IEEE Trans. Antennas Propag.*, vol. 60, no. 3, pp. 1312–1319, Mar. 2012.

[2] K. Kumar, J. S. Sandhu, B. Bisht, P. Gupta, and G. Singh, "Dual-band dielectric rod antenna for satellite communication system," in *Proc. Int. Conf. Commun. Syst. Netw. Technol.*, 2011, pp. 242–245.

[3] C.-C. Chen, K. Rama Rao, and R. Lee, "A new ultrawide-bandwidth dielectric-rod antenna for ground-penetrating radar applications," *IEEE Trans. Antennas Propag.*, vol. 51, no. 3, pp. 371–377, Mar. 2003.

[4] N. Ghassemi and K. Wu, "Planar dielectric rod antenna for gigabyte chip-to-chip communication," *IEEE Trans. Antennas Propag.*, vol. 60, no. 10, pp. 4924–4928, Oct. 2012.

[5] J. Richter, D. Notel, F. Kloppel, J. Huck, H. Essen, and L.-p. Schmidt, "A multi-channel radiometer with focal plane array antenna for W-band passive millimeterwave imaging," in *Proc. IEEE MTT-S Int. Microw. Symp. Dig.*, 2006, pp. 1592–1595.

[6] J.-H. Qiu and N.-N. Wang, "Optimized dielectric rod antenna for millimeter wave FPA imaging system," in *Proc. IEEE Int. Workshop Imag. Syst. Techn.*, 2009, pp. 147–150.

[7] W. Fang, P. Fei, and F. Nian, "Millimetre-wave end-fired antenna array for active 3D holographic imaging system," *Electron. Lett.*, vol. 50, no. 5, pp. 341–343, Feb. 2014.

[8] A. Elsherbini *et al.*, "UWB antipodal vivaldi antennas with protruded dielectric rods for higher gain, symmetric patterns and minimal phase center variations," in *Proc. IEEE Antennas Propag. Soc. Int. Symp.*, 2007, pp. 1973–1976.

[9] S. K. Mustafa and S. Yasir, "Design, development and testing of dielectric tapered rod feed for parabolic reflector antenna as an alternate to feed horns," in *Proc. 10th Int. Bhurban Conf. Appl. Sci. Technol.*, 2013, pp. 369–371.

[10] J. Y. Chung and C. C. Chen, "Two-layer dielectric rod antenna," *IEEE Trans. Antennas Propag.*, vol. 56, no. 6, pp. 1541–1547, Jun. 2008.

[11] R. B. Dyott, O. Lawn, and T. D. Monte, "Microwave transition using dielectric waveguides," *U.S. Patent 5 684 495*, Apr. 11, 1997.

[12] R. Kazemi, A. E. Fathy, and R. A. Sadeghzadeh, "Design guidelines for multi-layer dielectric rod antennas fed by Vivaldi antennas," *IET Microwaves, Antennas Propag.*, vol. 6, no. 8, pp. 884–892, Jun. 2012.

[13] C.-W. Liu, "Development of automatic design optimization method for ultrawide bandwidth (UWB) multi-layer dielectric rod antenna," *M.S. thesis*, Dept. Elect. Comput. Eng., Ohio State Univ., Columbus, OH, USA, 2011.

[14] Y. Luo and Z. N. Chen, "Compressed dipoles resonating at higher order modes with enhanced directivity," *IEEE Trans. Antennas Propag.*, vol. 65, no. 11, pp. 5697–5701, Nov. 2017.

[15] D. Lugo, R. A. Ramirez, J. Wang, and T. Weller, "Low permittivity cladding to improve the performance of dielectric rod waveguides and dielectric end-fire antennas," in *Proc. IEEE MTT-S Int. Microw. Symp.*, San Francisco, CA, USA, 2016.

[16] G. E. Mueller and W. A. Tyrrell, "Polyrod antennas," *Bell Syst. Tech. J.*, vol. 26, no. 4, pp. 837–851, Oct. 1947.

[17] T. Milligan, "Design of polyrod and corrugated-rod antennas," *IEEE Antennas Propag. Mag.*, vol. 42, no. 1, pp. 88–91, Feb. 2000.

[18] C. Balanis, *Antenna Theory Analysis and Design*, 3rd ed. Hoboken, NJ, USA: Wiley, 2005.

[19] D. C. Lugo, R. A. Ramirez, J. Castro, J. Wang, and T. M. Weller, "3D printed multilayer mm-wave dielectric rod antenna with enhanced gain," in *Proc. IEEE Int. Symp. Antennas Propag. USNC/URSI Nat. Radio Sci. Meeting*, San Diego, CA, USA, 2017.